Irreversible Photoreduction of Flavin in a Mutated Phot-LOV1 Domain†

Tilman Kottke,*,‡ Bernhard Dick,‡ Roman Fedorov,§,|| Ilme Schlichting,§,|| Rainer Deutzmann,⊥ and Peter Hegemann⊥

Institut für Physikalische und Theoretische Chemie, Universität Regensburg, Universitätsstrasse 31, 93053 Regensburg, Germany, Abt. Biophysikalische Chemie, Max Planck Institut für molekulare Physiologie, Otto Hahn Strasse 11, 44227 Dortmund, Germany, Abt. Biomolekulare Mechanismen, Max Planck Institut für medizinische Forschung, Jahnstrasse 29, 69120 Heidelberg, Germany, and Institut für Biochemie I, Universität Regensburg, Universitätsstrasse 31, 93053 Regensburg, Germany

Received May 22, 2003

ABSTRACT: Phot photoreceptors make up an important protein family regulating biological processes in response to blue light. They contain two light, oxygen, and voltage sensitive (LOV) domains and a serine/threonine kinase domain. Both LOV domains noncovalently bind a flavin mononucleotide (FMN). Upon absorption of blue light, the LOV domains undergo a photocycle, transiently forming a covalent adduct of a cysteine residue and the FMN (LOV-390). The mechanism of formation of this flavin−thiol adduct is still unclear. We studied a mutant of the LOV1 domain from the green alga *Chlamydomonas reinhardtii* with a methionine replacing the reactive cysteine 57 (C57M). As in the wild type, irradiation leads to formation of a photoadduct, which, however, is irreversibly converted into a red absorbing species, C57M-675. On the basis of spectroscopic results and the 2.1 Å resolution crystal structure, this highly unusual FMN species was assigned to a neutral flavin radical covalently attached to the apoprotein at the N(5) position. In contrast to other flavoprotein neutral radicals, C57M-675 is stable even under aerobic or denaturing conditions. Pathways for the photoinduced formation of the adduct are discussed for the C57M mutant as well as the wild-type LOV1 domain.

In 1998, phototropin of *Arabidopsis thaliana* was discovered as the first member of the fast growing "phot" protein family (*1*). Phot proteins are blue light photoreceptors regulating biological processes such as phototropic plant movement (*2*, *3*), chloroplast relocation (*4*−*6*), and stomatal opening in guard cells (*7*) as well as gametogenesis in green algae (*8*). Their common features are two light, oxygen, and voltage sensitive (LOV)[1] domains, each containing a noncovalently bound flavin mononucleotide (FMN), and a C-terminal kinase domain.

In the dark, the absorption spectra of the LOV domains exhibit two characteristic bands with vibrational fine structure. For the LOV1 domain from *Chlamydomonas reinhardtii*, the high-energy band is centered at 360 nm and the low-energy band at 447 nm (*9*, *10*). Following the conventions, the lowest energy maximum serves for the specification of spectroscopically distinguishable species (e.g., LOV1-447). Upon absorption of blue light, LOV domains undergo a photocycle (Figure 1) that tentatively activates a Ser/Thr kinase. The details of the photocycle and the signal transduction process are currently under investigation. Until now, two photocycle intermediates have been identified. The first

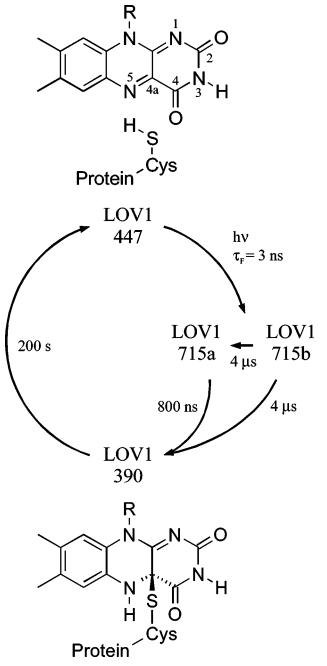

FIGURE 1: Photocycle of the Phot1-LOV1 domain from *C. reinhardtii* (adapted from ref *10*). Upon light absorption, the dark form LOV1-447 is converted into the triplet state LOV1-715. Two decay time constants implicate two triplet species with identical spectra. These decay into a flavin C(4a) cysteine adduct termed LOV1-390. The adduct is metastable and reverts to the dark form within minutes.

† This work was supported by the Deutsche Forschungsgemeinschaft (Grant GK 640).

* To whom correspondence should be addressed. Telephone: +49-941-943-4470. Fax: +49-941-943-4488. E-mail: tilman.kottke@chemie.uni-regensburg.de.

‡ Institut für Physikalische und Theoretische Chemie, Universität Regensburg.

§ Max Planck Institut für molekulare Physiologie.

|| Max Planck Institut für medizinische Forschung.

⊥ Institut für Biochemie I, Universität Regensburg.

[1] Abbreviations: EDTA, ethylenediaminetetraacetic acid; ENDOR, electron nuclear double resonance; EPR, electron paramagnetic resonance; ESI, electrospray ionization; FMN, flavin mononucleotide; LOV, light, oxygen, and voltage sensitive; SDS, sodium dodecyl sulfate; TCA, trichloroacetic acid; TLC, thin-layer chromatography.

10.1021/bi034863r CCC: $25.00
Published on Web 08/02/2003

intermediate with absorption maxima at 650 and 715 nm is present 30 ns after excitation and decays in the time range of microseconds (*10*, *11*). The intermediate has been assigned to the excited triplet state of the FMN (*11*). A second long-living intermediate is formed subsequently, which shows a broad absorption band with a maximum at 390 nm. Salomon et al. (*12*) proposed that the LOV-390 intermediate is a covalent adduct of the FMN and the apoprotein formed by the reaction of a conserved cysteine residue with the C(4a) atom of the flavin. This was verified by NMR spectroscopic studies (*13*) and X-ray crystallography (*14*, *15*). The LOV-390 intermediate is metastable and decays into the dark form within minutes.

The reaction pathway for the formation of LOV-390 is currently under debate. A clear deuterium isotope effect was observed for LOV2 from oat, suggesting that formation or breakage of bonds involving hydrogen atoms is a rate-limiting step (*16*).

A concerted mechanism was proposed by Crosson and Moffat (*17*) in which the N(5) position of the flavin is protonated as the thiol sulfur attacks C(4a). In a more detailed approach, Fedorov et al. (*15*) calculated the charge redistribution within the FMN upon formation of the triplet state based on the crystal structures of the LOV1 dark form (1.9 Å resolution) and the LOV1-390 flavin−thiol adduct (2.8 Å resolution). The negative charge on N(5) and the positive charge on C(5a) increase significantly, whereas C(4a) remains almost neutral. The authors suggested that during the lifetime of the triplet state the S−H proton moves toward the N(5) atom. Simultaneously, the extent of interaction of Cys57 with C(4a) increases until the sulfur orbitals overlap with those of C(4a) and the adduct is formed.

The first ionic mechanism starting from a deprotonated cysteine was proposed by Swartz et al. (*11*). The authors suggested that a flavin cation is formed by protonation of the FMN in the triplet state and is attacked by the thiolate anion. However, it has been shown by infrared spectroscopy on LOV2 from *Adiantum capillus-veneris* Phy3 (*18*) and LOV1 from *C. reinhardtii* Phot1 (*19*) that the reactive cysteine is protonated in the dark form. The corresponding S−H vibration mode disappears upon adduct formation. Thereupon, Crosson et al. (*20*) presented a reaction scheme in which base abstraction of the thiol proton by the excited FMN is followed by a nucleophilic attack of the sulfide. Spectroscopic analysis of the fine structure of the LOV2 absorption on a nanosecond time scale was taken as evidence of a protonated triplet state of the FMN (*21*).

For the concerted mechanism (*15*, *17*) and for the ionic pathway (*11*, *20*, *21*), the important step of triplet to ground state conversion has not been discussed. Neiss et al. (*22*) calculated the electron distribution for a complex of isolumazine and methanethiol as a model for the FMN−thiol complex of LOV domains on the basis of an *ab initio* formalism. From an energetic point of view, adduct formation in the triplet state is unlikely. The same authors favored a two-step radical mechanism starting with a hydrogen atom transfer from the cysteine to the FMN N(5) position followed by intersystem crossing and radical recombination. Likewise, Kay et al. (*23*) argued that adduct formation in the triplet state is unlikely. They favored the formation of a neutral flavin radical by initial electron transfer from the sulfur to the flavin and subsequent protonation. After intersystem crossing to the ground state, the semiquinone reacts with the cysteine radical to form the covalent adduct.

To clarify the adduct formation mechanism, we introduced a methylated thiol group into LOV1 from the *C. reinhardtii* Phot1. The replacement of the reactive cysteine with methionine (C57M) renders a proton or hydrogen atom transfer from the thiol group to the FMN impossible. We had expected that a photoreaction analogous to that of the wild type would lead to a stable LOV-390 intermediate with a methylated N(5) position, allowing further insight into the formation of the flavin C(4a)−thiol adduct.

However, the photoreaction of the C57M mutant resulted in a photoadduct that decayed on a time scale of hours into an unusual and extremely stable flavoprotein radical. The properties of the photoproducts were investigated by absorption spectroscopy, mass spectrometry, and X-ray crystallography. Further investigations on the radical species using electron paramagnetic resonance (EPR) and electron nuclear double resonance (ENDOR) are presented by Bittl et al. (*24*).

MATERIALS AND METHODS

LOV1 Expression and Purification. Wild-type Phot1-LOV1 from *C. reinhardtii* and the LOV1-C57S mutant were prepared as pMal fusion proteins as described previously (*10*). For the C57M mutant, cysteine 57 of wild type was exchanged for methionine by site-directed mutagenesis and amplified by overlapping PCR. The MBP−10His−LOV1-C57M fusion protein was expressed in *Escherichia coli* BL21(DE3), purified via amylose resin (New England Biolabs) (*10*), and stored at a concentration of 10 mg/mL in 10 mM potassium phosphate (pH 8.0) and 10 mM NaCl. For mass spectrometry, the fusion protein was dialyzed against 10 mM NaCl, 1 mM $CaCl_2$, and 50 mM Tris-HCl (pH 8.0) and cleaved with factor Xa (Roche) (1:100) for 3 days at room temperature. The His−LOV1-C57M fusion protein was finally purified via Ni−NTA column chromatography (Qiagen). The calculated average molar mass of the apoprotein is 14 963.0 g/mol. The wild-type sample for mass spectrometry was obtained as a 10His−LOV1 fusion protein using a pET16 vector (Novagen) (*10*).

Investigation of the LOV1-C57M Reaction Sequence. Absorption spectra were measured with a Lambda 9 spectrophotometer (Perkin-Elmer). The sample in its dark form was irradiated with a xenon flash (Metz 40-CT1) through a 435 nm cutoff filter (Schott GG435) until irradiation did not induce any further changes in the spectrum. The spectrum of C57M-415 obtained in this way showed a small contribution of secondary product C57M-675 and was therefore corrected by subtraction of the C57M-675 absorption. Full thermal conversion into C57M-675 was achieved by keeping the irradiated sample at 40 °C for up to 60 h. The kinetics of this conversion was derived from the spectral changes at 630 nm.

The relative quantum yield of C57M-415 formation in comparison to that of the wild type was obtained by measuring the loss in absorbance at 475 nm of the dark form after irradiation with a xenon flash through a 435 nm cutoff filter. Temperature, pH, volume, concentration, and path length were the same for wild-type and C57M mutant samples. In the case of the wild type, the bleaching directly after the flash was determined by a fit to the recovery kinetics. We assume that the FMN chromophores in the wild type and mutant have the same absorption coefficients.

For denaturation, sodium dodecyl sulfate (SDS) was added to the sample to a final concentration of 1% (total volume of 300 μL). The sample was subjected to ultrafiltration using

a filter with a 10 kDa molecular mass cutoff (Millipore Centricon YM-10) at a speed of 5000*g* until 40% of the total volume passed through the membrane. Small aliquots of the retentate and the filtrate were taken and diluted with phosphate buffer for analysis by absorption spectroscopy. The retentate was treated with trichloroacetic acid (TCA) to a concentration of 10%, and the precipitate was separated by centrifugation. Thin-layer chromatography (TLC) analysis of the supernatant was carried out in a solvent of butanol, acetic acid, and water (4:1:5).

Enzymatic digestion of C57M-675 was performed with a sample dialyzed against 10 mM Tris-HCl (pH 7.8), 5 mM ethylenediaminetetraacetic acid (EDTA), and 0.5% SDS. After proteinase K (Qiagen) was added to a concentration of 90 μg/mL, the sample was incubated at 45 °C for 20 h.

Photoreduction of LOV1-C57S. The neutral radical of the LOV1-C57S mutant was generated following standard procedures (*25*). The sample containing 100 mM phosphate buffer (pH 8) and 10 mM EDTA was made anaerobic by bubbling argon through the solution. The sample was irradiated with a 100 W tungsten lamp (Osram) through a 435 nm cutoff filter (Schott GG435). Absorption spectra were recorded until the absorbance at 570 nm reached its maximum.

Mass Spectrometry. Mass spectra were measured on a SSQ7000 single-quadrupole mass spectrometer (Thermo Finnigan), equipped with an electrospray ion (ESI) source. Sample solutions (2−5 μL) were introduced into the mass spectrometer via loop injection using a Rheodyne valve and a Harvard Apparatus microsyringe pump. The aqueous solution was delivered to the ESI source at a flow rate of 5−10 μL/min through a 75 μm fused silica capillary. The solvent was a methanol/water (1:1) mixture containing 0.5% acetic acid. The samples were dissolved in the same solvent at a concentration of ∼5−20 pmol/μL. The needle was positioned 5 mm from the capillary, and the capillary potential was set at 4.5 kV. The temperatures of the transfer capillary and the manifold were 100 and 220 °C, respectively. The pressure of the sheath gas (N_2) was 30 psi. It is typical for ESI to produce multiply charged protein ions. As a result, the mass spectra show a series of peaks corresponding to different *m*/*z* values, with neighboring peaks differing by one charge unit. From these data, the molecular mass of the protein can be calculated ("deconvolution"). This was done using the deconvolution program of the BioWorks software (Thermo Finnigan).

Crystallization and Structure Determination. LOV1-C57M was crystallized in the dark at 22 °C by vapor diffusion using the hanging drop geometry. One microliter of protein and reservoir solutions were mixed; the latter contained 100 mM Na^+-HEPES buffer (pH 7.3), 1.5−1.8 M ammonium sulfate, and 1−8% PEG8000. Yellow, pencil-shaped crystals grew after a couple of months. The cover slides with the hanging drops containing the crystals were placed for 20−40 s in front of a 100 W xenon lamp and then placed back atop the reservoir solutions. After 2−4 days, the now neon-green crystals were mounted in a loop and flash-cooled in liquid nitrogen. Diffraction data were collected at beamline ID14-2 at the ESRF (see Table 1 for details) using an ADSC Quantum 4 detector and were reduced with the XDS program package (*26*). The structure of the dark state of LOV1 (PDB entry 1N9L) was used as a starting model for refinement using CNS (*27*) and included simulated annealing and individual *B*-factor refinement. The topology and parameter files for the covalent Met57−FMN adduct were obtained from quantum chemical calculations (see ref *15*). During several cyclic rounds of refinement and manual rebuilding, a sulfate ion and solvent molecules were included in the model. The final model displays good stereochemistry (see Table 1).

Table 1: Statistics of Diffraction Data and Refinement for the Crystal Structure of C57M-675

crystal parameters	
$P6_522$ unit cell ($a = b$, c) (Å)	119.5, 45.6
data statistics	
resolution (Å)	15.0−2.1
no. of observations/no. of unique reflections	110224/11500
completeness (total/high) (%)[a]	98.5/99.7
$\langle I/\sigma(I)\rangle$ (total/high)[a]	18.2/7.1
R_{sym} (total/high)[a,b]	8.5/32.9
refinement statistics	
resolution range (Å)	8.0−2.1
included amino acids	17−125
no. of protein atoms	844
no. of waters	102
no. of SO_4^{2-} ions	1
R_{work}/R_{free} (%)[c]	18.6/21.9
rms deviation for bonds (Å)	0.007
rms deviation for angles (deg)	1.4

[a] Completeness, R_{sym}, and $\langle I/\sigma(I)\rangle$ are given for all data and for the highest-resolution shell (2.1−2.2 Å). [b] $R_{sym} = \sum|I - \langle I\rangle|/\sum I$. [c] $R_{work} = \sum|F_{obs}| - k|F_{calc}|/\sum|F_{obs}|$. Five percent of randomly chosen reflections were used for the calculation of R_{free}.

RESULTS

Dark Form of the LOV1-C57M Mutant. We employed a mutant of the LOV1 domain from the *C. reinhardtii* Phot1 receptor protein containing a methionine at position 57 (C57M) instead of the cysteine in the wild type. The absorption spectrum of the dark form of the C57M mutant is shown in Figure 2A. It closely resembles the spectrum of wild-type LOV1 with the difference of a less distinctly fine-structured absorption band at 350 nm. In the wild type as well as in the C57S mutant, at least two different vibrational transitions are visible in this spectral region (*10*). The main absorption maximum of C57M is slightly red-shifted to 448 nm compared with that of the wild type (447 nm).

Blue Light Induced Absorption Changes. Exposure of LOV1-C57M to blue light dramatically changed the absorption properties, indicating that the protein is photochemically reactive despite the mutation. The spectrum of the photoproduct (C57M-415) exhibits an absorption maximum at 350 nm and a broad shoulder around 415 nm (Figure 2B). The absorption properties resemble those of reduced flavin species (*28*).

In direct comparison to a wild-type sample, the efficiency of irradiation (i.e., bleaching) is reduced by a factor of 10 in the C57M mutant. The formed C57M-415 species proved to be more stable than the LOV1-390 product of the wild-type photoreaction. However, within several hours, it converted thermally into a species with unusually red-shifted absorption. For conversion at 40 °C, the time constant was 4 h. The spectrum of the thermoproduct (Figure 2C) contains two absorption maxima in the red part of the spectrum (675 and 625 nm) and three maxima in the blue region (450, 370, and 320 nm). This C57M-675 species was stable for several months under aerobic conditions.

Photoactivation Links the Chromophore FMN Irreversibly to the Protein. In wild-type LOV1 and in the LOV1-C57M

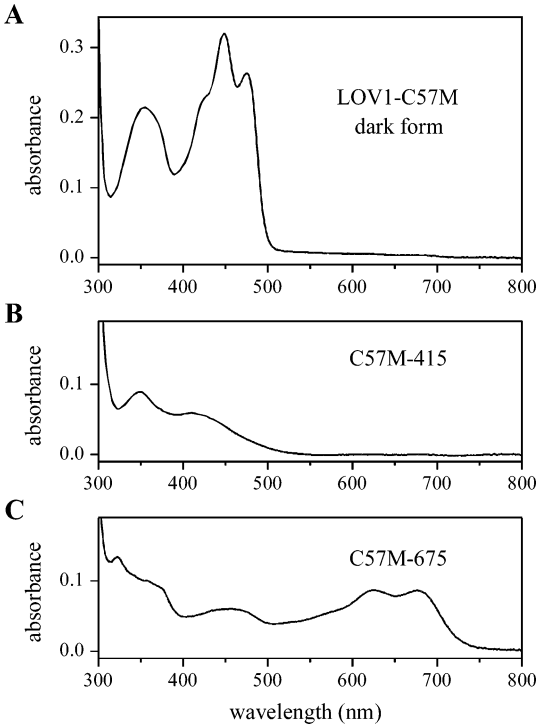

FIGURE 2: Sequence of absorption spectra showing the stepwise reaction of the C57M mutant. The C57M dark form (A) is converted upon blue light irradiation into the photoproduct C57M-415 (B). Thermal conversion of C57M-415 leads to the final reaction product C57M-675 (C).

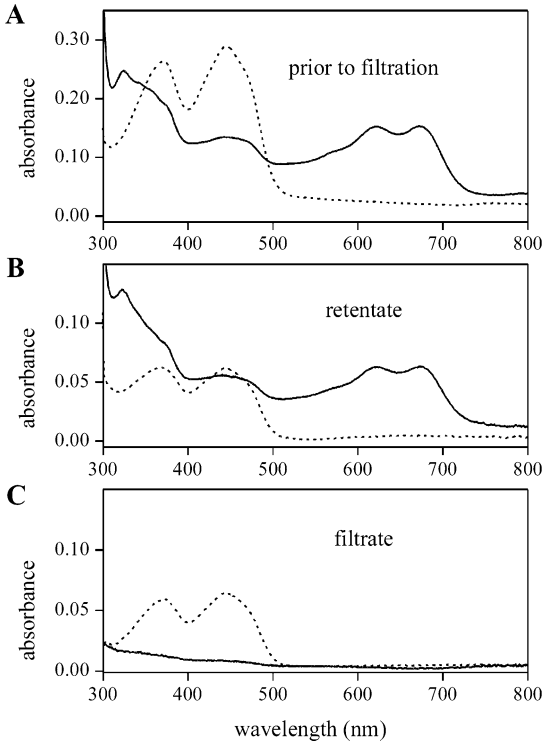

FIGURE 3: Ultrafiltration and analysis by absorption spectroscopy of denatured samples of C57M-675 (—) and wild-type LOV1 (···). The spectra prior to ultrafiltration (A) and of the retentate (B) show the absorption of C57M-675 and of free FMN. In the filtrate (C) (40% of the total volume), the chromophore of C57M-675 is not detectable, indicating that it cannot be separated from the apoprotein. The retentate and filtrate were diluted for analysis.

dark form, denaturation caused a loss of fine structure of the FMN absorption band around 450 nm obviously due to relief of protein-induced conformational constraints and exposure of the FMN to the aqueous bulk phase (Figure 3A). Surprisingly, in C57M-675, the absorption properties of FMN were influenced very little by chromophore−protein interaction. Denaturation in 1% SDS or 8 M urea did not change the absorption maximum, and in particular, the fine structure of the long-wavelength absorption band was left unchanged. Ultrafiltration could not separate the FMN chromophore from the denatured C57M-675 protein, which was easily possible in denatured wild-type LOV1 (Figure 3). Only complete removal of the protein environment by digestion with proteinase K led to a loss of the C57M-675 absorption. Similarly, upon precipitation of C57M-675 in TCA, the chromophore was released from the protein and exhibited the characteristic absorption of an oxidized FMN in TCA. The identity with the FMN was supported by TLC analysis.

To confirm a covalent linkage between the FMN and the apoprotein, we investigated the photoreaction sequence of C57M by electrospray ionization (ESI) mass spectrometry. The deconvoluted mass spectrum (see Materials and Methods) of the C57M dark form exhibits a main peak at a mass of 14 959 Da (Figure 4A). On the basis of the calculated mass of 14 963.0 g/mol, the signal can be assigned to the apoprotein. Accompanying peaks at masses of an extra 76 and 98 units may be attributed to traces of sodium and phosphate ions, respectively, aggregating with the protein. Irradiation with blue light, which promotes formation of C57M-415, increased the protein mass by 460 units to 15 419 Da (Figure 4B). The increase of 460 units after irradiation is in good agreement with the mass of the FMN chromophore (456 g/mol). This allows the conclusion that FMN is covalently linked to the protein in the photoproduct C57M-

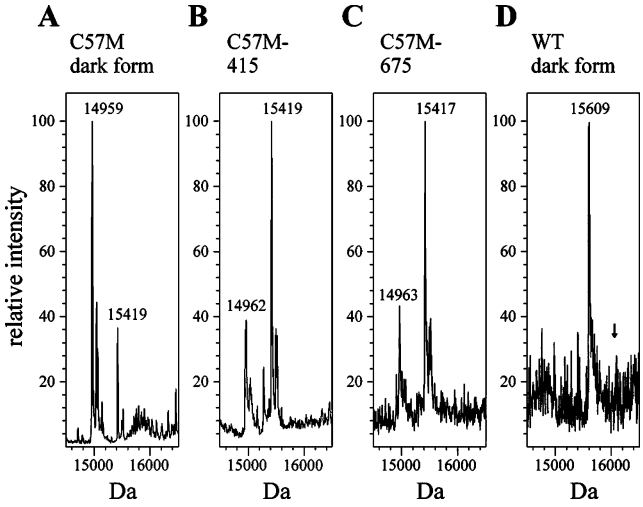

FIGURE 4: Deconvoluted ESI mass spectra of the C57M photoreaction sequence. The main mass signal of the C57M dark form (A) can be attributed to the apoprotein. The photoproduct C57M-415 (B) exhibits an increase in mass of 460 units, indicating a covalent binding of the FMN to the apoprotein. Thermal conversion to C57M-675 (C) has no further effect on the signal pattern. For comparison, the wild-type spectrum (D) shows the signal of the wild-type apoprotein (cloned into a different vector; see ref *10*). The arrow marks a mass increase of 460 units where no signal is present in the spectrum.

415. Due to incomplete conversion, the signal of the apoprotein is still present in the spectrum of C57M-415. The mass pattern of the heat-treated protein, C57M-675, is shown in Figure 4C. It does not reveal any change relative to C57M-415. Again, this result supports the earlier proposal of a

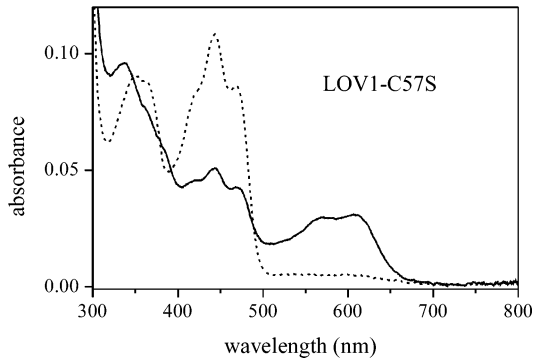

FIGURE 5: Irradiation of the LOV1-C57S mutant in the presence of EDTA under anaerobic conditions. The dotted line shows the absorption spectrum of the sample before exposure to light. The solid line depicts the characteristic features at 570 and 610 nm of a flavoprotein neutral radical species generated by blue light irradiation.

covalent linkage of FMN to the protein in C57M-675, but does not clarify how both partners had reacted. For comparison, the wild-type dark form (His-tagged) was investigated and exhibits a peak at 15 609 Da (Figure 4D), in agreement with the calculated mass for the wild-type apoprotein (*10*). No further signals are present in the wild-type spectrum. The second signal in the C57M dark form spectrum at 15 419 Da (Figure 4A) can therefore be assigned to the photoadduct C57M-415, formed by exposure to faint light during the preparation process.

Comparison of C57M-675 with a Neutral Flavoprotein Radical of the C57S Mutant. Usually, absorption bands of flavin species in the red spectral region either are due to charge transfer complexes or can be attributed to flavin radicals. Electron paramagnetic resonance (EPR) studies on C57M-675 yielded a signal that is characteristic of a neutral flavin radical species (*24*). Most flavoproteins can be converted into radicals by irradiation under anaerobic conditions in the presence of a reducing agent, such as EDTA (*25*). We used a LOV1 mutant in which cysteine 57 was replaced with serine (C57S) to prevent thiol adduct formation (*10*). Blue light irradiation of LOV1-C57S in the presence of 10 mM EDTA generated a species with absorption maxima at 570 and 610 nm (Figure 5). Upon admission of air, the initial spectrum of the unexposed sample was regained. The spectrum resembles that of a typical neutral flavoprotein radical (*23*, *25*). In contrast, the spectrum of C57M-675 is significantly red-shifted by 65 nm.

Crystal Structure of C57M-675. To analyze the covalent linkage between the apoprotein and the FMN chromophore as well as the associated conformational changes within the protein, LOV1-C57M was crystallized according to the procedure established for wild-type LOV1 (*15*). The pencil-shaped crystals were illuminated and kept for 2−4 days at room temperature for conversion into C57M-675. Since the crystals of the long-lived radical species are isomorphous with those of the wild type, the structure was determined by difference Fourier methods. The overall three-dimensional structure of C57M-675 is very similar to that of the wild-type LOV1 in the dark state (PDB entry 1N9L), with a C_α rms deviation of 0.2 Å. Except for the flexible N-terminus and residues D50 and E51 forming a loop of α-helix 2 that participates in a crystallographic contact, C_α traces of both structures are practically identical. The only noticeable differences in conformations of side chains are observed for surface residues E63, K68, E69, Q71, K72, R74, K78, K79, R86, and R112 that are not stabilized by intramolecular interactions. There is a difference in the positions of the C(5*) and O(5*) atoms of the FMN ribityl chain, whereas the rest of the chain and the phosphate have not changed. Most of the active site residues (including the M57 region) have the same conformations as their analogues in the dark state structure of wild-type LOV1. There are only two exceptions. The L34 and Q120 side chains appear to be shifted to prevent overly close contacts with the atoms of the M57 side chain in C57M-675. As shown in Figure 6, there is clear electron density for a covalent link between the mutated M57 and N(5) of the isoalloxazine ring. The isoalloxazine ring essentially preserves its flat conformation. The conformation of the M57 side chain in C57M-675 is not strained. A nice fit to the experimental electron density can be achieved by two small rotations around the methionine $C_\alpha-C_\beta$ and $S_\delta-C_\epsilon$ bonds starting from one of the standard rotamers. This explains why formation of a covalent bond between the terminal carbon atom of the methionine side chain and the N(5) atom of the isoalloxazine ring does not cause any changes in the M57-containing region.

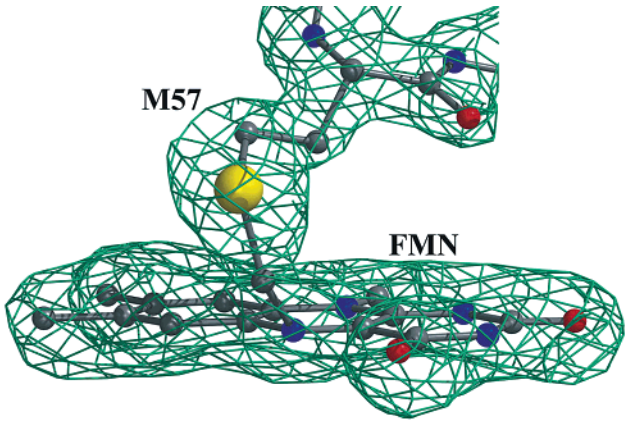

FIGURE 6: Close-up view of the chromophore pocket obtained from the crystal structure of C57M-675 showing the covalent linkage between flavin and methionine. Depicted is the $2F_o - F_c$ omit electron density map contoured at 1.3σ around the positions of FMN and Met57.

DISCUSSION

Upon absorption of blue light, LOV1-C57M undergoes a photoreaction despite the exchange of the reactive cysteine for methionine. We propose a reaction sequence as depicted in Figure 7. After excitation to the triplet state, the flavin reacts with the terminal methyl group of methionine, forming the adduct C57M-415. In a subsequent thermal reaction, the adduct is oxidized to the final reaction product, the radical C57M-675. In the following, we will discuss the evidence for this proposal and present a mechanistic view of the photoreaction.

Spectral Features of the Reduced Flavin Species C57M-415. The spectrum of C57M-415 with two absorption bands at 350 and 415 nm closely resembles spectra of reduced flavoproteins (*28*). For comparison, the wild-type thiol adduct LOV1-390 exhibits a single broad absorption band at 390 nm (*10*), whereas this single band is blue-shifted to 340−360 nm in N(5)- and C(4a)-alkylated reduced flavins (*29*). The 350 nm absorption of C57M-415 is therefore in agreement with an alkylation of the reduced FMN (Figure 7). The presence of a second electronic transition at >400 nm is an indication of a coplanar geometry of reduced flavins

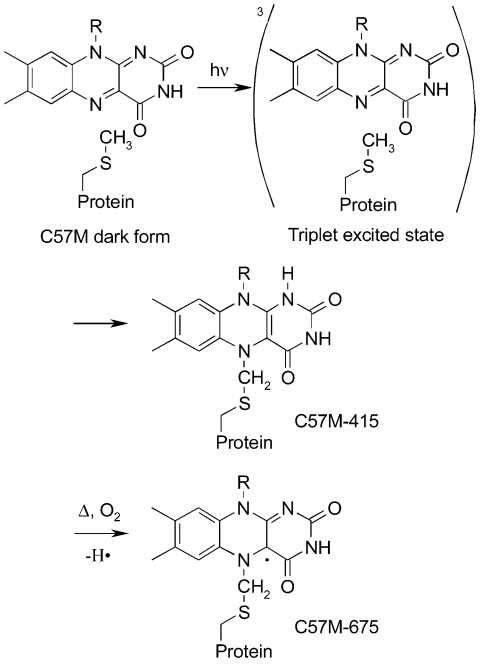

FIGURE 7: Photoreaction of the LOV1-C57M mutant. After excitation of the FMN to the triplet state, its reaction with the terminal methyl group of methionine leads to formation of the photoadduct C57M-415. Slow thermal oxidation of the adduct generates the neutral flavoprotein radical C57M-675.

(*30*) and a measure for the degree of sp2 hybridization of N(5) (*31*). A single absorption band is accordingly explained by a predominantly sp3-hybridized N(5) in C(4a) and N(5) adducts. In N(5) adducts, this is caused by a "butterfly" conformation with an N(5)−N(10) bending axis (*31*). The presence of the 415 nm band in C57M-415 allows us to conclude that the photoadduct is substituted at the N(5) position and possesses a fairly planar conformation enforced by the protein environment and the steric repulsion between the N(5) and N(10) substituents. Similarly, the proton has to be localized at N(1) and not at the C(4a) position. An additional presence of a C(4a)-alkylated adduct cannot be evaluated on the basis of the spectrum.

C57M-675 Is a Flavoprotein Radical with a Covalently Bound Chromophore. The prominent absorption of C57M-675 in the red spectral region provokes a comparison with three well-known flavin species.

(1) The triplet state of free FMN shows a fine-structured band with maxima at 660 and 710 nm (*32*). Similar spectra were observed for the FMN triplet state of LOV2 from *Avena sativa* (*11*) and LOV1 from *C. reinhardtii* (*10*). However, the lifetime of the triplet state in the time domain of microseconds excludes the assignment of C57M-675 to a triplet state.

(2) Charge transfer complexes of flavin with adjacent protein residues may lead to absorption in the red spectral range. To the best of our knowledge, these charge transfer complexes appear as broad absorption bands with single maxima (*33*) and do not show the fine structure of C57M-675. Because charge transfer complexes are based on negative charges close to the FMN π-system, the absorption is lost upon protein denaturation.

(3) Neutral radical species of flavoproteins are characterized by their absorption at 590 and 620 nm (*25*). In LOV1-C57S from *C. reinhardtii*, the neutral radical is formed by an electron transfer from EDTA to the excited FMN presumably via one or more redox-active amino acids and protonation. In contrast, in C450A-mutated LOV2 from *A. sativa*, a neutral radical is formed by illumination already in the absence of any external electron donor (*23*). A red shift of more than 50 nm distinguishes the latter species from C57M-675. Anionic flavoprotein radicals are not considered because they absorb at 490 nm (*25*).

The extreme red shift of C57M-675 may be explained by alkylation of the FMN at the N(5) position. Spectra of free N(5)-ethyl flavin neutral radicals are indeed similar to the C57M-675 spectrum (*34*). More direct evidence for the radical nature of C57M-675 is provided by EPR and ENDOR measurements (*24*).

Mechanistic Proposal for the C57M Photoreaction. A reaction sequence for C57M analogous to that of the wild type would lead to a flavin C(4a)-homocysteine adduct that is methylated at the N(5) position. The homolytic cleavage of such a S−C(4a) linkage would result in an N(5)-methylated radical species that is disconnected from the apoprotein and released upon protein denaturation. However, this mechanism is refuted by mass spectrometry (Figure 4). The electron density in the crystal structure of C57M-675 (Figure 6) shows a linkage between the apoprotein and the FMN composed of the methionine side chain (C−S−C) attached to N(5). The structure clearly indicates a reaction of the terminal hydrocarbon of the methionine with the FMN instead of the cysteine sulfur in the wild type.

For the first step in the wild-type reaction, base abstraction of the thiol proton by the excited FMN has been proposed (*20*, *21*). In the C57M mutant, the thiol proton has been replaced with a methyl group and water molecules or acidic amino acids are not present in the vicinity of the chromophore (*15*). Thus, protons are most likely not available for protonation of the N(5) position of flavin. An abstraction of a proton from a terminal thiomethyl group and formation of a carbanion are unlikely from an energetic point of view. A two-step ionic mechanism for adduct formation can therefore be ruled out for the mutant reaction. However, a concerted mechanism (*15*, *17*) is feasible and will be discussed elsewhere (R. Fedorov, unpublished experiments). Neiss et al. (*22*) and Kay et al. (*23*) favor a radical mechanism for wild-type adduct formation, because the other proposals implicate a quantum mechanically unlikely bond formation during the triplet lifetime. It has already been discussed controversially for decades by Heelis (*35*) or Hemmerich (*36*) whether flavin photoreduction in general is proceeding via one- or two-electron transfer, respectively. Interestingly, indications for radical intermediates have already been found in spectroscopic studies on LOV1 (*10*) and LOV2 (*21*), but the latter authors questioned their relevance for adduct formation. In conclusion, we favor a radical mechanism to explain the reactions occurring in both the wild type and C57M mutant (Figure 8).

We propose that after excitation of the FMN chromophore to the triplet state, a hydrogen atom is abstracted from the terminal methyl group of the methionine. The hydrogen transfer is facilitated via a primary one-electron transfer from the sulfur atom of methionine to the flavin, followed by a subsequent transfer of a proton (see also ref *24*). A primary electron transfer was proposed by Yang et al. (*37*) for the reaction of free methionine with FMN. Hydrogen abstraction from the CH_2 group next to the sulfur is also conceivable but was excluded on the basis of the crystal structure. The resulting flavin neutral radical **A** and the reactive $S-CH_2^{\bullet}$

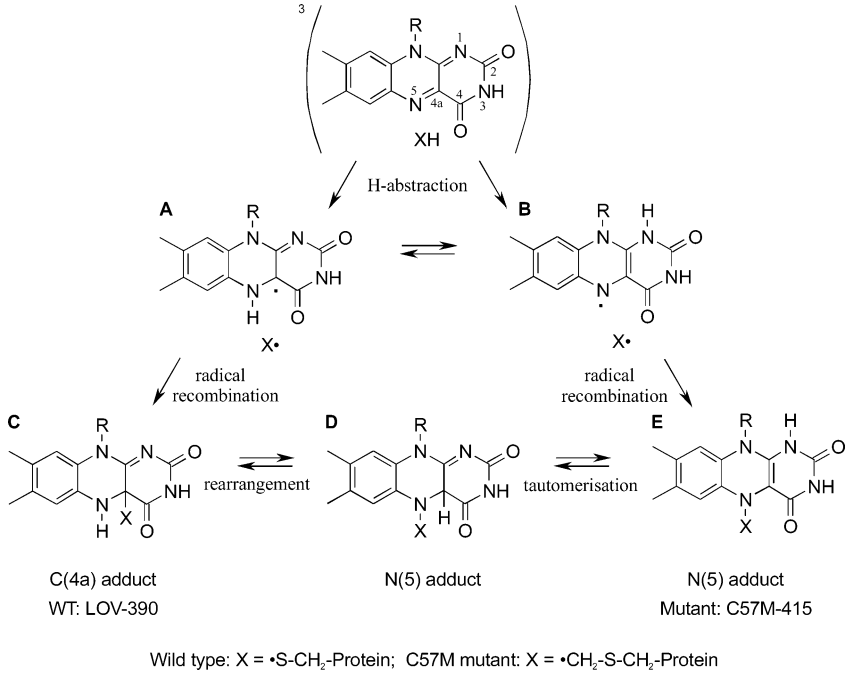

FIGURE 8: Pathways of the photoreaction of the C57M mutant and wild-type LOV1 domain proposing a radical mechanism. In the wild type, abstraction of a hydrogen atom from the cysteine generates radical **A**. Radical recombination leads to C(4a) adduct **C** (LOV-390). In the mutant C57M, abstraction of a hydrogen from the terminal methyl group of methionine is similarly followed by formation of adduct **C**, but a rearrangement to N(5) adduct **E** takes place (C57M-415), most likely via intermediary adduct **D**. Alternatively, C57M-415 might be generated directly via isomeric radical species **B**. The thermal back reaction in the wild type and the radical formation in the C57M mutant were omitted for clarity.

group recombine under formation of a flavin C(4a) adduct **C**. This kind of radical addition reaction has been proposed by Heelis after observation of flavin radicals in flash-photolysis studies with amino acids as substrates (*35*). In the mutant, however, a subsequent rearrangement to N(5) adduct **E** must take place (C57M-415). This step is energetically favorable as is shown by computational studies presented in the Appendix. For free flavin in solution, it has been found that C(4a) and N(5) adducts can be interconverted via a rearrangement (*29*), with the position of the equilibrium depending on reaction conditions and substitution. In the case of thioethers, the final product is the N(5) adduct (*38*). In the photoreaction of FMN with methionine in LOV1, N(5) adduct **E** is formed accordingly (C57M-415), most likely via intermediary N(5) adduct isomer **D**. In the presence of oxygen, the photoadduct is slowly oxidized to the stable flavin radical C57M-675, as described for N(5) adducts by Walker and Hemmerich (*29*). This is in agreement with the finding that the mass signal of C57M-675 is unchanged compared to that of C57M-415.

An alternative, direct pathway needs to be discussed. Neutral radical **B** bearing a proton at the N(1) position is not much higher in energy than N(5)-protonated species **A**, as shown in the Appendix. Other isomers with protons at O(4) or C(4a) can be ruled out. Partially populated radical **B** might recombine with the amino acid radical and directly form final N(5) adduct **E** (C57M-415). This would imply an early separation between mutant and wild-type reaction mechanisms.

The reduction of the quantum yield of C57M adduct formation by a factor of 10 compared to the yield of the wild type can be explained by the change in the reactivity from a thiol group in the wild type to a hydrocarbon in the mutant. In line with our mechanistic proposal, both abstraction of a hydrogen atom as well as transfer of an electron and subsequent deprotonation are rendered more difficult by replacing a cysteine thiol with a methionine thiomethyl group.

Unusual Stability of the Radical C57M-675. Most flavoprotein radicals are rather stable under anaerobic conditions but rapidly react with molecular oxygen. One of the few exceptions is the neutral flavin radical in *E. coli* DNA photolyase (*39*). The protein environment prevents disproportionation and may also stabilize the radical via hydrogen bonding but usually does not prevent the reaction with oxygen (*40*, *41*). In contrast, C57M-675 is stable under aerobic conditions for months. This may be caused by the stabilizing effect of N(5) alkylation as has been reported for free flavin radicals (*41*). But surprisingly, C57M-675 does maintain the fine-structured absorption bands even under denaturing conditions where the C57M dark form releases the chromophore from the apoprotein. The covalent bond between the FMN and protein obviously guarantees protection of the radical in SDS or urea. This is a clear difference from other flavoprotein radicals that are considered stable. For example, in *E. coli* DNA photolyase, the flavin radical decays immediately in 0.8% SDS already under anaerobic conditions (*39*). Similarly, the neutral flavoprotein radical generated in the LOV1-C57S mutant (Figure 5) survived only under exclusion of oxygen. C57M-675, however, decays only under very acidic conditions, when the radical converts into free oxidized FMN. Dealkylation might occur via protonation of the radical followed by oxidation and hydrolysis of the unstable radical cation (*42*).

ACKNOWLEDGMENT

We thank Tina Schiereis for excellent technical assistance and Eduard Hochmuth for recording the mass spectra. We also thank Elisabeth Hartmann for crystallizing LOV1-C57M

Table 2: Total Energies E and Energy Differences ΔE Obtained by Geometry Optimization Calculations for Several Intermediates Discussed in the Photoreduction of FMN in the Wild Type and the C57M Mutant of LOV1[a]

	species	AM1 E (kcal/mol)	HF/6-31G E (au)	AM1 ΔE (kJ/mol)	HF/6-31G ΔE (kJ/mol)
radical	**A** [FMN•-N(5)-H]	1.67	−828.0331398	0.0	0.0
	B [FMN•-N(1)-H]	4.55	−828.0311941	12.0	5.1
	FMN•-O(4)-H	12.81	−828.0156014	46.6	46.0
	FMN•-C(4a)-H	26.19	−827.9901231	102.6	112.9
adduct (X = SCH_3)	**C** [C(4a) adduct]	−0.68	−1265.1035822	0.0	0.0
	D [N(5) adduct]	2.61	−1265.0731625	13.8	79.9
	E [N(5) adduct]	3.52	−1265.0949867	17.6	22.6
adduct (X = CH_2SCH_3)	**C** [C(4a) adduct]	−5.74	−1304.1201641	0.0	0.0
	D [N(5) adduct]	3.17	−1304.1084222	37.3	30.8
	E [N(5) adduct]	−9.74	−1304.1304144	−16.7	−26.9

[a] The radical species were produced by attachment of a hydrogen atom to the indicated atom. The adduct species correspond to structures **C**−**E** shown in Figure 8. Model compounds for the formation of the adduct of FMN with the S−H bond of cysteine bear SCH_3 as X (wild type). Species with CH_2SCH_3 as X are the corresponding models for adducts to the C−H bond of methionine (C57M mutant).

and Christian Neiss and Tatiana Domratcheva for stimulating discussions.

APPENDIX

To explore the feasibility of the radical mechanism presented in Figure 8, we performed quantum mechanical calculations. The first step of this mechanism is the abstraction of a hydrogen atom by the FMN triplet, either from the S−H group of cysteine or from the S−CH_3 group of methionine. The second step is the formation of a bond between the FMN•-H radical and the amino acid radical X•. If the hydrogen atom is attached to N(5) of FMN and the radical X• to C(4a), the result is adduct **C** known from the wild type (LOV-390). Structure **E** that we assign to the C57M-415 state of the C57M mutant may be formed by attachment of the hydrogen atom to N(1) of FMN followed by a combination of the radical X• with N(5). Alternatively, structure **C** may be formed first, in analogy with the wild-type reaction. This may then be followed by a rearrangement into structure **E**, most likely via intermediate **D**.

We have used the AM1 method (*43*) for fast geometry optimization of the FMN•-H radical as well as of model compounds for the FMN−protein adducts. FMN was modeled by 7,8-dimethyl-N(10)H-isoalloxazine, cysteine by H-SCH_3, and methionine by H-CH_2SCH_3. Four isomers of each product were considered. The resulting structures were used as input to an *ab initio* geometry optimization on the HF/6-31G level. Calculations were performed using the PC GAMESS version (*44*) of the GAMESS (US) QC package (*45*). The results are collected in Table 2.

Comparison of four isomers of the FMN•-H radical shows that in the most stable radical **A** the hydrogen is located at N(5), in agreement with experimental findings (*40*). N(1)-protonated radical **B** is only slightly higher in energy and might be populated to some extent at room temperature. Furthermore, the calculations predict that the hydrogen abstraction by triplet FMN leading to radical **A** is exothermic not only for the hydrogen donors cysteine and methionine but also for serine (data not shown). Since adduct formation with serine is not observed (*10*), we conclude that the direct hydrogen transfer has a high barrier and that the system takes an alternative route involving electron transfer followed by proton transfer. The calculated ionization energy of serine is indeed much larger than that of cysteine and methionine. In the series of model compounds for the cysteine adduct, structure **C** corresponding to the experimentally observed structure is more stable than structures **D** and **E** (Table 2). For the model compounds of the methionine adduct, however, species **E** is more stable than **C** and **D**. This result supports our assignment of the C57M-415 adduct.

Both computational methods AM1 and HF/6-31G come to the same conclusion about the relative stabilities of the FMN•-H radicals as well as those of structures **C** and **E** of the adduct models. For the formation of wild-type adduct **C**, this supports a simple two-step mechanism in which the most stable species is formed in every step. If the same route is followed by the C57M mutant, exothermic isomerization to species **E** is expected to follow as a third step. Alternatively, **E** might be formed directly if species **B** is the reactive FMN•-H radical. According to both calculations, the energy difference between FMN•-H radicals **A** and **B** is so small that species **B** might be sufficiently populated at room temperature to allow a direct reaction of LOV1-C57M.

REFERENCES

1. Christie, J. M., Reymond, P., Powell, G. K., Bernasconi, P., Raibekas, A. A., Liscum, E., and Briggs, W. R. (1998) *Arabidopsis* NPH1: a flavoprotein with the properties of a photoreceptor for phototropism, *Science 282*, 1698−1701.
2. Liscum, E., and Briggs, W. R. (1995) Mutations in the NPH1 locus of *Arabidopsis* disrupt the perception of phototropic stimuli, *Plant Cell 7*, 473−485.
3. Huala, E., Oeller, P. W., Liscum, E., Han, E., Larsen, I. S., and Briggs, W. R. (1997) *Arabidopsis* NPH1: A protein kinase with a putative redox-sensing domain, *Science 278*, 2120−2123.
4. Kagawa, T., Sakai, T., Suetsugu, N., Oikawa, K., Ishiguro, S., Kato, T., Tabata, S., Okada, K., and Wada, M. (2001) *Arabidopsis* NPL1: a phototropin homolog controlling the chloroplast high-light avoidance response, *Science 291*, 2138−2141.
5. Jarillo, J. A., Gabrys, H., Capel, J., Alonso, J. M., Ecker, J. R., and Cashmore, A. R. (2001) Phototropin-related NPL1 controls chloroplast relocation induced by blue light, *Nature 410*, 952−954.
6. Sakai, T., Kagawa, T., Kasahara, M., Swartz, T. E., Christie, J. M., Briggs, W. R., Wada, M., and Okada, K. (2001) *Arabidopsis* nph1 and npl1: blue light receptors that mediate both phototropism and chloroplast relocation, *Proc. Natl. Acad. Sci. U.S.A. 98*, 6969−6974.
7. Kinoshita, T., Doi, M., Suetsugu, N., Kagawa, T., Wada, M., and Shimazaki, K. I. (2001) Phot1 and phot2 mediate blue light regulation of stomatal opening, *Nature 414*, 656−660.
8. Huang, K., and Beck, C. F. (2003) Phototropin is the blue-light receptor that controls multiple steps in the sexual life cycle of the green alga *Chlamydomonas reinhardtii*, *Proc. Natl. Acad. Sci. U.S.A. 100*, 6269−6274.
9. Holzer, W., Penzkofer, A., Fuhrmann, M., and Hegemann, P. (2002) Spectroscopic characterization of flavin mononucleotide bound to the LOV1 domain of Phot1 from *Chlamydomonas reinhardtii*, *Photochem. Photobiol. 75*, 479−487.
10. Kottke, T., Heberle, J., Hehn, D., Dick, B., and Hegemann, P. (2003) Phot LOV1: Photocycle of a blue light receptor domain from the green alga *Chlamydomonas reinhardtii*, *Biophys. J. 84*, 1192−1201.

11. Swartz, T. E., Corchnoy, S. B., Christie, J. M., Lewis, J. W., Szundi, I., Briggs, W. R., and Bogomolni, R. A. (2001) The photocycle of a flavin-binding domain of the blue light photoreceptor phototropin, *J. Biol. Chem. 276*, 36493−36500.
12. Salomon, M., Christie, J. M., Knieb, E., Lempert, U., and Briggs, W. R. (2000) Photochemical and mutational analysis of the FMN-Binding Domains of the Plant Blue Light Receptor, Phototropin, *Biochemistry 39*, 9401−9410.
13. Salomon, M., Eisenreich, W., Dürr, H., Schleicher, E., Knieb, E., Massey, V., Rüdiger, W., Müller, F., Bacher, A., and Richter, G. (2001) An optomechanical transducer in the blue light receptor phototropin from *Avena sativa*, *Proc. Natl. Acad. Sci. U.S.A. 98*, 12357−12361.
14. Crosson, S., and Moffat, K. (2002) Photoexcited structure of a plant photoreceptor domain reveals a light-driven molecular switch, *Plant Cell 14*, 1067−1075.
15. Fedorov, R., Schlichting, I., Hartmann, E., Domratcheva, T., Fuhrmann, M., and Hegemann, P. (2003) Crystal structures and molecular mechanism of a light induced signaling switch: the Phot-LOV1 domain from *Chlamydomonas reinhardtii*, *Biophys. J. 84*, 2474−2482.
16. Corchnoy, S. B., Swartz, T. E., Lewis, J. W., Szundi, I., Briggs, W. R., and Bogomolni, R. A. (2003) Intramolecular proton transfers and structural changes during the photocycle of the LOV2 domain of Phototropin 1, *J. Biol. Chem. 278*, 724−731.
17. Crosson, S., and Moffat, K. (2001) Structure of a flavin-binding plant photoreceptor domain: Insights into light-mediated signal transduction, *Proc. Natl. Acad. Sci. U.S.A. 98*, 2995−3000.
18. Iwata, T., Tokutomi, S., and Kandori, H. (2002) Photoreaction of the cysteine S-H group in the LOV2 domain of *Adiantum* phytochrome3, *J. Am. Chem. Soc. 124*, 11840−11841.
19. Ataka, K., Hegemann, P., and Heberle, J. (2003) Vibrational spectroscopy of an algal Phot-LOV1 domain probes the molecular changes associated with blue-light reception, *Biophys. J. 84*, 466−474.
20. Crosson, S., Rajagopal, S., and Moffat, K. (2003) The LOV domain family: Photoresponsive signaling modules coupled to diverse output domains, *Biochemistry 42*, 2−10.
21. Kennis, J. T. M., Crosson, S., Gauden, M., van Stokkum, I. H. M., Moffat, K., and van Grondelle, R. (2003) Primary reactions of the LOV2 domain of phototropin, a plant blue-light receptor, *Biochemistry 42*, 3385−3392.
22. Neiss, C., and Saalfrank, P. (2003) *Ab initio* quantum chemical investigation of the first steps of the photocycle of phototropin: a model study, *Photochem. Photobiol. 77*, 101−109.
23. Kay, C. W. M., Schleicher, E., Kuppig, A., Hofner, H., Rüdiger, W., Schleicher, M., Fischer, M., Bacher, A., Weber, S., and Richter, G. (2003) Blue light perception in plants. Detection and characterization of a light-induced neutral flavin radical in a C450A mutant of phototropin, *J. Biol. Chem. 278*, 10973−10982.
24. Bittl, R., Kay, C. W. M., Weber, S., and Hegemann, P. (2003) Characterization of a flavin radical product in a C57M mutant of a LOV1 domain by electron paramagnetic resonance, *Biochemistry 42*, 8506−8512.
25. Massey, V., and Palmer, G. (1966) On the existence of spectrally distinct classes of flavoprotein semiquinones. A new method for the quantitative production of flavoprotein semiquinones, *Biochemistry 5*, 3181−3189.
26. Kabsch, W. (1993) Automatic processing of rotation diffraction data from crystals of initially unknown symmetry and cell constants, *J. Appl. Crystallogr. 26*, 795−800.
27. Brunger, A. T., Adams, P. D., Clore, G. M., DeLano, W. L., Gros, P., Grosse-Kunstleve, R. W., Jiang, J. S., Kuszewski, J., Nilges, M., Pannu, N. S., Read, R. J., Rice, L. M., Simonson, T., and Warren, G. L. (1998) Crystallography and NMR system: A new software suite for macromolecular structure determination, *Acta Crystallogr. D54*, 905−921.
28. Ghisla, S. (1974) Fluorescence and optical characteristics of reduced flavins and flavoproteins, *Biochemistry 13*, 589−597.
29. Walker, W. H., and Hemmerich, P. (1970) Light-induced alkylation and dealkylation of the flavin nucleus, *Eur. J. Biochem. 13*, 258−266.
30. Dudley, K. H., Ehrenberg, A., Hemmerich, P., and Müller, F. (1964) Spektren und Strukturen der am Flavin-Redoxsystem beteiligten Partikeln, *Helv. Chim. Acta 47*, 1354−1383.
31. Moonen, C. T. W., Vervoort, J., and Müller, F. (1984) Reinvestigation of the structure of oxidized and reduced flavin: Carbon-13 and nitrogen-15 nuclear resonance study, *Biochemistry 23*, 4859−4867.
32. Sakai, M., and Takahashi, H. (1996) One-electron photoreduction of flavin mononucleotide: time-resolved resonance Raman and absorption study, *J. Mol. Struct. 379*, 9−18.
33. Williams, C. H., Jr. (1992) Lipoamide dehydrogenase, glutathione reductase, thioredoxin reductase, and mercuric ion reductase: a family of flavoenzyme transhydrogenases, in *Chemistry and Biochemistry of Flavoenzymes* (Mueller, F., Ed.) Vol. III, pp 121−211, CRC Press, Boca Raton, FL.
34. Nanni, E. J., Jr., Sawyer, D. T., Ball, S. S., and Bruice, T. C. (1981) Redox chemistry of N5-ethyl-3-methyllumiflavinium cation and N5-ethyl-4a-hydroperoxy-3-methyllumiflavin in dimethylformamide. Evidence for the formation of the N5-ethyl-4a-hydroperoxy-3-methyllumiflavin anion via radical−radical coupling with superoxide ion, *J. Am. Chem. Soc. 103*, 2797−2802.
35. Heelis, P. F. (1982) The photophysical and photochemical properties of flavins (isoalloxazines), *Chem. Soc. Rev. 11*, 15−39.
36. Hemmerich, P. (1976) The present status of flavin and flavocoenzyme chemistry, *Fortschr. Chem. Org. Naturst. 33*, 451−527.
37. Yang, S. F., Ku, H. S., and Pratt, H. K. (1967) Photochemical production of ethylene from methionine and its analogues in the presence of flavin mononucleotide, *J. Biol. Chem. 242*, 5274−5280.
38. Knappe, W. R., and Hemmerich, P. (1976) Reductive photoalkylation of the flavin nucleus; structure und reactivity of the photoproducts, *Liebigs Ann. Chem. 11*, 2037−2057.
39. Jorns, M. S., Sancar, G. B., and Sancar, A. (1984) Identification of a neutral flavin radical and characterization of a second chromophore in *Escherichia coli* DNA photolyase, *Biochemistry 23*, 2673−2679.
40. Müller, F., Hemmerich, P., Ehrenberg, A., Palmer, G., and Massey, V. (1970) The chemical and electronic structure of the neutral flavin radical as revealed by electron spin resonance spectroscopy of chemically and isotopically substituted derivatives, *Eur. J. Biochem. 14*, 185−196.
41. Müller, F., Brüstlein, M., Hemmerich, P., Massey, V., and Walker, W. H. (1972) Light-absorption studies on neutral flavin radicals, *Eur. J. Biochem. 25*, 573−580.
42. Walker, W. H., Hemmerich, P., and Massey, V. (1970) Light-induced alkylation and dealkylation of the flavin nucleus. Stable dihydroflavins: spectral course and mechanism of formation, *Eur. J. Biochem. 13*, 258−266.
43. Stewart, J. J. P. (1990) *MOPAC*, version 6.0, Frank J. Seiler Research Laboratory, United States Air Force Academy, Colorado Springs, CO.
44. Granovsky, A. A. (2003) http://classic.chem.msu.su/gran/gamess/index.html.
45. Schmidt, M. W., Baldridge, K. K., Boatz, J. A., Elbert, S. T., Gordon, M. S., Jensen, J. H., Koseki, S., Matsunaga, N., Nguyen, K. A., Su, S., Windus, T. L., Dupuis, M., and Montgomery, J. A. (1993) General atomic and molecular electronic structure system, *J. Comput. Chem. 14*, 1347−1363.

BI034863R